

An integrated approach for the HCl and metals recovery from waste pickling solutions: pilot plant and design operations

R. Gueccia¹, D. Winter², S. Randazzo¹, A. Cipollina^{1*}, J. Koschikowski², G. Micale¹

¹Dipartimento di Ingegneria, Università degli studi di Palermo, Palermo, 90128, Italy

²Fraunhofer Institute for Solar Energy Systems ISE, 79110 Freiburg, Germany

*Corresponding author: e-mail: andrea.cipollina@unipa.it

ABSTRACT

Continuous regeneration of industrial pickling solutions and recovery of valuable materials are implemented in a pilot-scale plant including diffusion dialysis (DD), where HCl is recovered, membrane distillation (MD), where HCl is concentrated, and reactive precipitation (CSTR), where metal ions are recovered in different forms. The integration of the three processes allows to minimize waste streams generation and to accomplish a closed-loop process, thus increasing the environmental sustainability and economic impact of the galvanizing industry. Process reliability was proved through the operation of a demonstrator plant in the real industrial environment of the Tecnozinco SrL (Carini, Italy) hot-dip galvanizing plant, assessing the actual performances in fully reducing spent pickling solution disposal and in terms of recovered compounds quality. Tests were conducted firstly with artificial solutions and then with real waste liquors from the pickling plant. A high acid recovery (80%) can be achieved in the Diffusion Dialysis unit and quantitative metals separation was achieved, with iron hydroxide produced at 99% purity. The membrane distillation performances suffer when metal salts are present in large quantities due to the “salting out” effect resulting in reduced water vapor pressure, though, the use of available low grade waste heat allows energy-sustainable operation of MD.

KEYWORDS: industrial wastewater; acid recovery; membrane technologies; demonstrator, circular economy.

1 INTRODUCTION

Hot-dip zinc galvanizing is one of the leading technologies used worldwide for steel rustproofing, with pickling being a determinant step of the whole process chain. The pickling process is a metal surface treatment, which consists in dipping corroded steel products into acidic baths, mainly hydrochloric acid solution, to remove impurities, oxides and scale. Pickling baths are batch reactors, in which the iron oxides layers from steel products are degraded by the acid attack with the subsequent acid consumption and iron oxides conversion into iron (II) chlorides (Jatuphaksamphan et al., 2010). Indeed, pickling bath composition continuously changes. According to Kleingarn (Kleingarn, 1988), optimal pickling conditions given by acid and iron concentration combination can be identified in which oxide dissolution is faster and pickling efficiency is maximized (Campano, 2012). Hence the importance of continuously controlling acid and iron composition in the bath in order to optimise the pickling process.

Currently, pickling baths are stressed until the acid concentration decreases by 75-85% and the metals concentration reaches the highest solubility threshold (Campano, 2012). Then, they are discharged as spent pickling solution (SPS), thus quitting optimal performances for most of the bath working life. SPS discharge has a dramatic impact in the industry economics as well as in the ecological footprint. In the EU alone, up to 300.000 m³ year⁻¹ of SPS is produced (Frias et al., 1997). This leads to a high ecologic and economic burden and significant room for improvement has been recently identified (Kong and White, 2010).

The complexity of treating solutions from a pickling bath is related to the fact that these are mixtures of numerous inorganic and organic compounds.

Extended scientific research, in more than 40 years of studies and applications on this topic, has focused mainly on the treatment of the pickling waste at the end of its life. Although several alternative methods of recovering exhausted solutions have been proposed, few applications of demonstrator plants are reported in the literature (Balakrishnan et al., 2018). Balakrishnan et al.

investigated three different technologies at the demonstrator scale: diffusion dialysis, acid retardation and nanofiltration. Behind the several issues encountered in the industrial application, the waste solution was very low acid concentrated, since disposal solutions were considered, and the treatment benefit were focused on the acid recovery, thus only minimizing the waste production, which will in any case undergo through a further neutralization step.

A well-known and established technology for the acid regeneration is the spray roasting (Bascone et al., 2016; Harris, 1994) process. The ANDRITZ Group has proposed their own recovery technology based on spray roasting and fluid bed processes (Andritz Metals) with several applications located worldwide.

However, the engineering complexity and the harsh operating conditions (high temperature and corrosive gases) of these technologies makes their applications suitable only for large-scale metallurgical plants (Harris, 1994). The main drawbacks is that they are very energy intensive (Devi et al., 2014; Stocks et al., 2005) and they suffer for the presence of zinc in solution, due to the formation of low melting compounds at the high process working temperature (Kerney, 1994).

On the other hand, the solvent extraction (Regel et al., 2001) and the ion-exchange resins (Marañón et al., 2000) technologies, which are able to separate metals too, require an high-energy and chemicals consumption and significant investment and operating costs (Kerney, 1994).

The aim of this work is to provide an innovative hybrid technology for both minimizing the waste production of metallurgical industry by recycling and recovering valuable products, and optimizing the pickling process through the continuous control of pickling baths composition.

The challenge is proofing the continuous regeneration of the pickling bath and the optimal bath composition control by means of the testing and operation of a demonstrator pilot-scale plant installed and operated at the Tecnozinco (Carini, PA, Italy) hot-dip galvanizing plant.

In this case, the stream to be treated is not exhausted pickling solution at the end of its life, but a stream with still high performance level, from which metals are partially removed and acid is recovered.

The integrated process feasibility and design have been studied and proposed through the application of a process simulator (Culcasi et al., 2019) and it is made up of three different processes: a diffusion dialysis (DD), a membrane distillation (MD) and a reactive precipitation unit (CSTR).

The diffusion dialysis process is very compelling for its clean nature and operational simplicity, low installation and operating costs and low energy consumption (Luo et al., 2011; Xu et al., 2009), such a lot to be compatible with BAT recommendations (European Commission, 2006). Compared to other membrane technologies, such as electrodialysis or reverse osmosis, the diffusion dialysis process does not operate with electrical potential or pressure difference across the membrane. The DD process is governed by transport phenomena driven by concentration gradients of chemical species present on either side of the membranes. Indeed, in our case, waste acid and softened low grade tap water are used as process streams, respectively. The acid diffuses across the membrane into the deionised water, whereas metals are blocked by the anion exchange membrane (AEM) due to their positive charge (Strathmann, 2004). Plenty of studies are available in literature for the single DD unit application as pickling waste treatment process (Balakrishnan et al., 2018; Kobuchi et al., 1986; Tongwen and Weihua, 2003). Research efforts have been committed to investigate how the acid recovery efficiency is influenced by the common metals components (Jung Oh et al., 2000; Luo et al., 2013) (e.g. FeCl_2 , ZnCl_2 , NiCl_2) and promising finding for the acid recovery were obtained (Gueccia et al., 2020, 2019). For the HCl pickling system, it was found out that iron chlorides provide additional chlorides in solution enhancing the acid passage (Gueccia et al., 2019; Luo et al., 2013). Conversely, zinc ions in acid solution are mainly present as negative chloro-complexes, which act as competitor

for the acid recovery, thus reducing the acid passage (Gueccia et al., 2020; Jung Oh et al., 2000; Palatý and Žáková, 2006).

The membrane distillation is a thermally driven separation process with applications in acid concentration of pickling waste (Tomaszewska et al., 2001). Temperature and composition gradients generate a vapour pressure difference across the two sides of a hydrophobic microporous membrane resulting in vapour molecules passage from the hot to the cool channel. Metal salts components are non-volatile compounds hence massive rejection is achievable. Unfortunately, HCl is a volatile compound and, indeed, the liquid-vapour equilibrium is influenced from both the temperature and concentration of acid and salts in the feed (Tomaszewska et al., 2001, 1998). What really attracts in the use of MD is the possibility of using low grade thermal energy, thus enabling the application of industrial waste heat (Drioli et al., 1987). Taking into account the harsh environment created due to the acids, the MD module applied in the present study is a feed gap air gap membrane distillation (FGAGMD) (Schwantes et al., 2019); here the aggressive media is only in contact with the feed and permeate channels, which are hydraulically separated from the channels that supply heating and cooling. As a consequence, normal water can be used as heat transfer fluid, significantly reducing the potential risk and costs dedicated to the thermal sub-system.

In order to accomplish the circular reuse of all the process streams and, at the same time, the minimization of the environmental impact, heavy metals from the solution leaving the DD are separated in a precipitation step. Chemical reactants, specifically hydrogen peroxide and ammonium hydroxide (i.e. ammonia) solution, are required for the precipitation process of this pilot study. Nevertheless, by-products are generated from the reaction: i) the $ZnCl_2$ and NH_4Cl solution, as it can provide a part of the industrial fluxing solution consumed in the plant; ii) and a nearly pure iron hydroxide solid product, with a marketable value (e.g. in painting industry or in wastewater treatment plants (Zhao et al., 2015)). This approach also overcomes the main

limitation of traditional neutralisation with hydroxides (NaOH or Ca(OH)₂) consisting in the co-precipitation of different metals, thus preventing from the achievement of high purity precipitates (Agrawal and Sahu, 2009; Kerney, 1994).

Finally, worth noting that, in addition to the environmental friendly and low energy consumption aspects, membrane technologies can be easily scaled-up thus making the present pilot demonstrator study a very useful example for possible industrialisation analysis.

2 PILOT PLANT AND OPERATIONAL PROCEDURES

2.1 Demonstrator

The demonstrator unit has been designed based on the output of a simulation campaign (Culcasi et al., 2019) and assembled in all its parts at Fraunhofer Institute for Solar Energy Systems, Freiburg, Germany. The unit has been subsequently installed and operated in real environment at Tecnozinco SrL in Carini (Sicily, Italy). The plant for the treatment of waste acid solutions was designed for testing the innovative approach for the recovery of hydrochloric acid and iron, recycling the remaining zinc metal solution, thus reducing the waste water disposal and guaranteeing continuous optimal conditions of the pickling process. The plant consists of three different core processes: recovery of free acid, concentration of recovered acid, recovery of iron salts and zinc solution. The detailed illustration of the process is presented in the simplified process flow diagram (PFD) shown in Figure 1, for which the meaning of abbreviations is explained throughout the relevant text and reported in the “Nomenclature, acronyms and units” section.

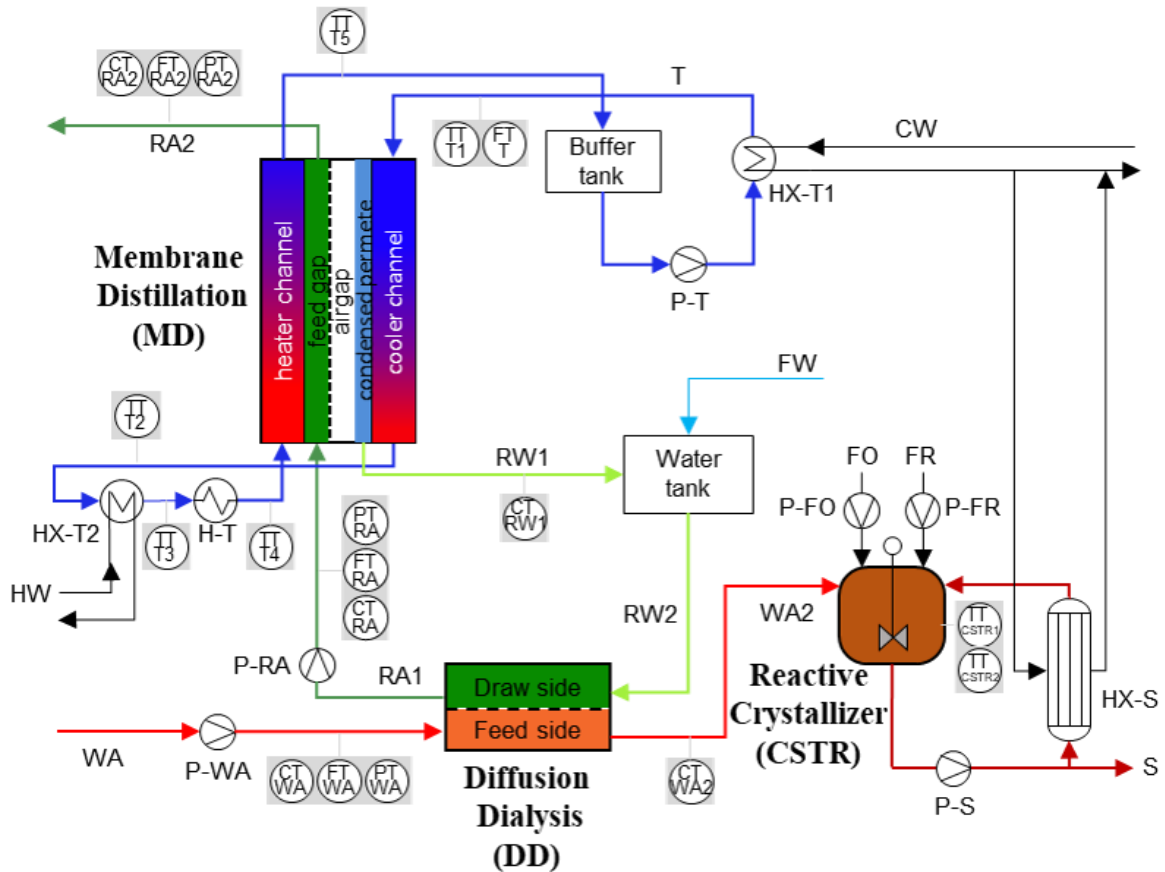


Fig. 1. Simplified process flow diagram of the demonstrator plant.

The self-priming electrically-controlled membrane pump P-WA (KNF Neuberger GmbH, Freiburg, Germany) primes the pre-treated waste acid solution (WA) through the DD module. The DD module has a plate and frame configuration, designed and manufactured by DEUKUM GmbH (Frickenhäusen, Germany). Detailed DD module characteristics are reported in Table 1. The feed side of the DD module is flushed vertically against gravity from the bottom to the top. In the opposite side, a draw solution, which is a mixture of slightly acidic recovered water (RW2) and softened fresh water (FW), is sucked from the P-RA pump (KNF Neuberger GmbH, Freiburg, Germany), flowing from top to bottom thus realizing a countercurrent arrangement in the DD unit. The free acid permeates through the anion exchange membranes from the feed to the draw solution thanks to the concentration gradient, while the metal ions are predominantly rejected by the membrane. As a consequence, the feed solution loses its acid concentration and

increases the metals ions concentration when exiting the DD module (WA2), while the diffusate solution exits the module with an increased acid concentration (RA1) and some metal ions, which have overcome the membrane rejection capacity.

The recovered acid stream RA1 is pumped from P-RA into the feed channel of the MD module, in which water is extracted by the thermally-driven evaporation process. The MD module has a plate and frame configuration with a feed gap/air gap configuration (Schwantes et al., 2019). Technical specification of the MD module (Solar Spring GmbH, Freiburg, Germany) are reported in Table 1. The driving force for the process is related to the temperature difference across the membrane, which is guaranteed by a heat-transfer fluid flowing in the thermostatic line (T), consisting in softened tap water recirculating in a closed loop by a controlled centrifugal pump P-T (Iwaki Europe GmbH, Willich, Germany). The thermostatic line allows to cool-down one side of the MD module and heat-up the other one, being itself heated/cooled by the two service heat exchangers, HX-T1 and HX-T2 (Kelvion, Bochum, Germany), respectively. An electrical heater H-T (Siekerkotte, Herford, Germany) is also included in the hydraulic circuit as “emergency” heater to be used when waste heat is not available. Due to the water extraction in the MD module, the acidic stream is concentrated leaving the MD-module on the top side, from which it can be recirculated to the pickling bath following an adjustment with make-up hydrochloric acid (at 34% w/w). By varying temperature and flowrates in the MD-module, the rate of concentration can be controlled. Finally, the water vapour extracted condenses on the cold surface of the air gap channel of the module and is cycled back as recovered water (RW1) into the product water tank. Due to the partially volatile behaviour of HCl, a relevant acid drag over into the extracted product water is also observed.

The metals rich brine (WAS2) exiting from the DD process is fed into the crystallizer (CSTR) (features reported in Table 1). The iron II in solution (FeCl_2) is oxidized to iron III (FeCl_3) by the addition of hydrogen peroxide (FO) via dosing pump P-FO (KNF Neuberger GmbH,

Freiburg, Germany), operating with an accurate control of the redox potential in the tank. Simultaneously, the reactive precipitation of $\text{Fe}(\text{OH})_3$ is induced by the addition of ammonium hydroxide solution (FR) via dosing pump P-FR (KNF Neuberger GmbH, Freiburg, Germany)), producing a $\text{Fe}(\text{OH})_3$ slurry in the CSTR tank. Since the oxidation of FeCl_2 is exothermic, the slurry is recirculated through a polymer tube bundle heat exchanger HX-S (Calorplast, Krefeld, Germany) via a pneumatic membrane pump P-S (Jessberger GmbH, Ottobrunn, Germany), allowing the continuous cooling of the crystallizer. Zinc ions remain in solution together with ammonium chlorides, due to their higher precipitation pH value (in the form of zinc hydroxide). Solids are separated from the slurry via filtration, and the filtered solution can be reused in the pickling process within the fluxing bath, where a zinc/ammonium chloride solution is used. Conversely, the separated solid particles of $\text{Fe}(\text{OH})_3$ are dried and sold to the market.

The plant energy sustainability is achieved also by using the waste heat as primary energy source for the MD process. The plant is connected hydraulically to the local heating water network (HW), which is fed from available waste heat originating from the hot zinc bath.

The cooling requirements for the MD process as well as for the exothermic reactions in the CSTR, are guaranteed via the cooling water (CW) loop, which discard excess heat via a PP-lined aluminium coil placed inside the scrubber unit of the industrial plant.

The total footprint of the demonstrator plant is $2.4 \times 1.4 \text{ m}^2$ (with a height of 2.1 m). The resulting weight is 1.5 tons when empty, while when full of liquid up to 1.8 tons.

Process	Technical specifications		
DD	N° membranes	94	-
	Channel length	0.8	m
	Channel width	0.2	m
	Channel thickness	270	μm
	Total membrane area	15	m^2
	Residence time	7	min
MD	N° parallel stages	2	-
	Channel length	4.32	m
	Channel width	0.72	m
	Feed/Distillate channel thickness	0.002	m

	Heater/Cooler channel thickness	0.004	m
	Total membrane area	6.22	m ²
	Residence time	45	min
CSTR	Reactor height	0.4	m
	Maximum liquid level	0.35	m
	Reactor diameter	0.3	m
	Paddle diameter	0.2	m
	Capacity	25	l
	Impeller rotation speed	400	rpm
	Residence time	1	min

Table 1. Technical specifications of the main process units.

In Figure 2 the front and back sides of the demonstrator plant are illustrated, highlighting the main technologies.

The whole process is controlled through integrated loops allowing to control all main operating variables, within a highly automatized system based on the use a SIEMENS SIMATIC human machine interface (HMI). Some pictures of the demonstrator plant at the Tecnozinco industrial site and examples of HMI display captures are also showed in Figure 2.

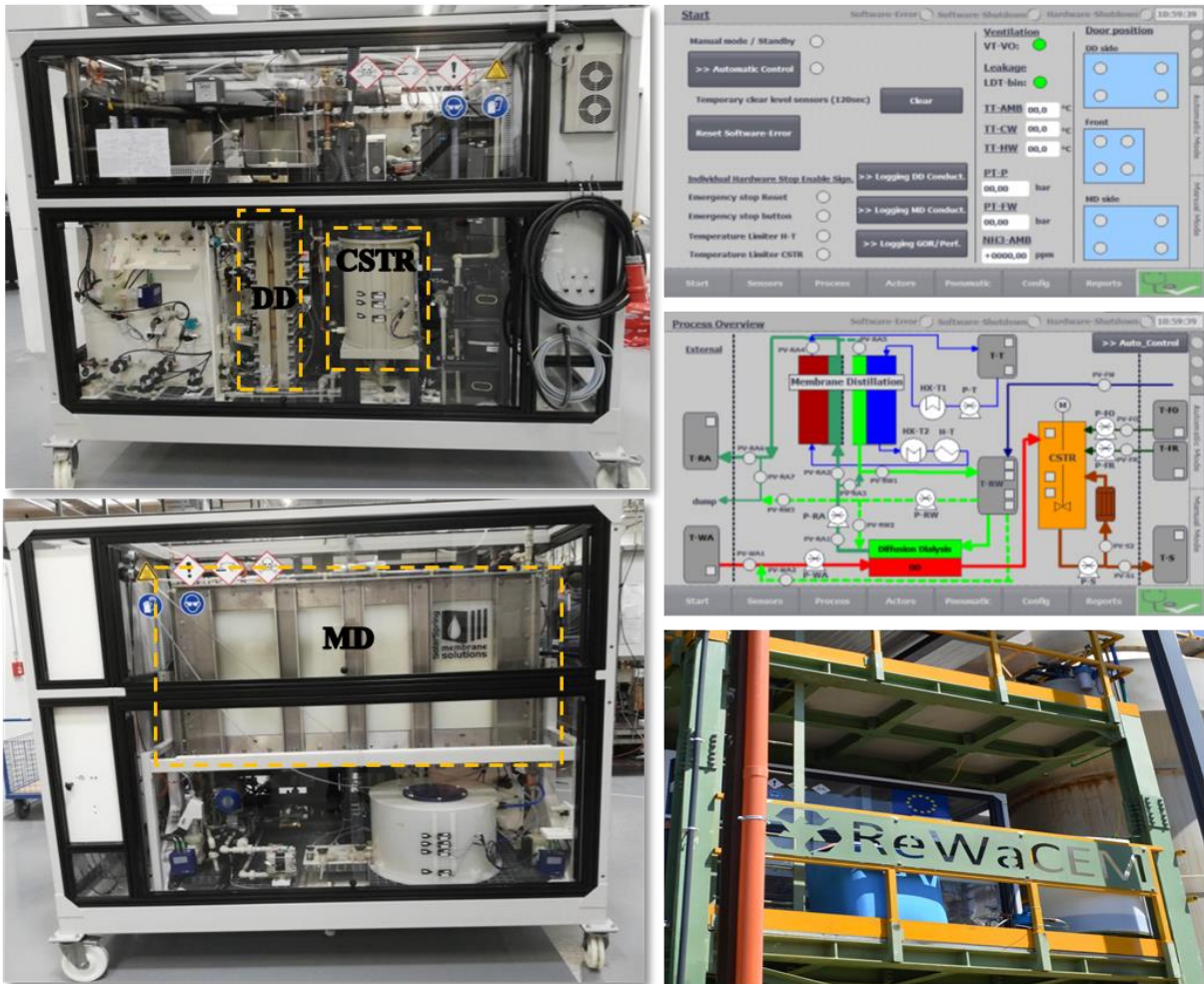


Fig. 2. Front and back views of the demonstrator plant (left side): (DD) diffusion dialysis, (CSTR) reactive precipitation, (MD) membrane distillation; HMI displays captures and photo of the demonstrator plant installed at Tecnozinco SrL, Carini, Italy (right side).

2.2 Materials and Methods

Tests were conducted with a stepwise approach, by performing preliminary experiments with artificial solution of HCl and then operating the system with real pickling liquors. In the latter case, solutions were initially prepared through the pickling of iron pieces in an acid tank. The prepared solution underwent a simple filtration step with cartridge (10 μm) before being fed to the pilot process line. In a second stage, also pickling solutions from the real industrial baths were used after being treated through a demulsifier / oil separator and a subsequent activated carbon filter for the removal of surfactants and residual organics.

Results were processed and presented in terms of key performance indicators, as described in the following.

For the DD process, the acid recovery ratio (RR_{DD}) and metals leakage ($Metals\ Leakage_{DD}$) were monitored, each one defined as:

$$RR_{DD}(\%) = \frac{F_{RA1} \cdot c_{HCl,RA1} - F_{RW2} \cdot c_{HCl,RW2}}{F_{WA} \cdot c_{HCl,WA}} \times 100 \quad (1)$$

$$Metals\ Leakage_{DD}(\%) = \frac{F_{RA1} \cdot c_{(Fe;Zn),RA1} - F_{RW2} \cdot c_{(Fe;Zn),RW2}}{F_{WA} \cdot c_{(Fe;Zn),WA}} \times 100 \quad (2)$$

where F is the volumetric flow rate, c the bulk concentration of the acid and metals components; RA1, RW2 and WA subscripts stand for recovered acid from DD, recovered water; and waste acid, respectively.

MD performances are assessed through the Gain Output Ratio (GOR), the acid drag over ($Acid\ drag\ over_{MD}$) and the permeate flux ($RW1\ flux$).

GOR , identifying the thermal efficiency of the evaporative process, is defined as:

$$GOR = \frac{F_{RW1} \cdot \rho_{water} \cdot \Delta h_v}{\dot{Q}_{heat}} \quad (3)$$

where RW1 subscript stands for water vapor extracted from MD, $\Delta h_v (=2257\text{ kJ kg}^{-1})$ is the enthalpy of evaporation, $\rho_{water}=997\text{ kg m}^{-3}$ and \dot{Q}_{heat} is the heating power, calculated as:

$$\dot{Q}_{heat} = F_T \cdot cp \cdot (T_{T4} - T_{T2}) \quad (4)$$

with $cp (=4.19\text{ kJ kg}^{-1}\text{ K}^{-1})$ being the specific heat, $(T_{T4} - T_{T2})$ the temperature difference between condenser outlet and evaporator inlet and T subscript the thermostatic fluid.

The GOR can be read also as a measure of the thermal integration of the system as it shows the ratio between the energy needed for the permeate evaporation and the energy supplied externally ideally in the form of saturated condensing vapor.

The acid drag over ($Acid\ drag\ over_{MD}$) and the permeate flux ($RW1\ flux$) are defined as:

$$Acid\ drag\ over_{MD}(\%) = \frac{F_{RW1} \cdot C_{HCl,RW1}}{F_{RA1} \cdot C_{HCl,RA1}} \times 100 \quad (5)$$

$$RW1\ flux = \frac{F_{RW1}}{A_{MD}} \quad (6)$$

where A_{MD} is the effective MD membrane area.

Finally, CSTR performance was assessed by the measure of solid $Fe(OH)_3$ purity:

$$Fe(OH)_3\ purity(\%) = \frac{m_{Fe}^{analysis}}{m_{Fe}^{theor}} \times 100 \quad (7)$$

where $m_{Fe}^{analysis}$ is the fraction of Fe, detected in the solid sample (after filtration, drying and dissolution in stoichiometric quantities plus 10% excess of HCl solution at $1\ mol\ l^{-1}$) by spectrophotometric analysis ; m_{Fe}^{theor} is the theoretical amount of iron in the sample, assuming that this contains only iron hydroxide.

2.3 Analysis

Conductivity monitoring of the different process lines was performed with in-line conductivity sensors (JUMO CTI-750, Sesto San Giovanni, Italy). The acid concentration was measured by titration with a standard titrant Na_2CO_3 solution (Carlo Erba, Val-de-Reuil, France $\geq 99.5\%$) and methyl orange solution 0.1% as indicator (Carlo Erba, Val-de-Reuil, France). Iron ions concentration was detected by spectrophotometry (Beckham DU 800 spectrophotometer, Brea, CA, US) by adding 1,10-phenanthroline monohydrate (Sigma Aldrich, St. Louis, MO, US, $\geq 99\%$) and characterizing the samples at of 510 nm wavelength. Zinc ions concentration was measured by atomic absorption using a Shimadzu AA6200 absorption spectrophotometer (Shimadzu, Kyoto Japan).

Flow rates through all relevant sections of the plant were measured with MIB Flowmax 400i (MIB GmbH, Breisach, Germany). Temperature monitoring, was realized through the TC PT 100 temperature sensor (TC direct Mönchengladbach, Germany), while a double security

temperature transmitter TT-CSTR1/2 (JUMO, Sesto San Giovanni, Italy), which initiates the plant security hardware shutdown, was adopted for the CSTR temperature.

Worth noting that each experiment presented in this work was repeated at least 2 times in order to estimate statistical errors reported in the graphs as error bars.

3 RESULTS AND DISCUSSION

In Table 2, for the sake of clarity, all the relevant investigated operating conditions for the tests performed with the demonstrator plant and discussed in details in Section 3.1 to 3.3, are summarized.

Test type	Variable operating parameters	WA-FT [l h ⁻¹]	RA-FT [l h ⁻¹]	T-FT [l h ⁻¹]	T-TT [°C]	WA inlet concentration		
						C _{HCl} [g l ⁻¹]	C _{Fe} [g l ⁻¹]	C _{Zn} [g l ⁻¹]
Test with HCl solution (artificial)	WA and RA flow rate	15	19	400	60	100	-	-
		25	15					
		20	21					
	T flowrate and temperature	20	19	300	60			
				400				
				500				
				300	70			
				400				
				500				
Test with HCl and Fe solution (real)	WA and RA flow rate	15	15	300	60	100	80	-
		20	19					
		25	21					
Test with HCl, Fe and Zn solution (real)	Fe concentration	20	19	300	60	100	44	8
							117	

Table 2. Summary of all tests performed for the demonstrator in the industrial environment along with the operating parameters varied for sensitivity analysis.

3.1 Preliminary tests with artificial HCl solutions

The demonstrator was first commissioned in “safe” operational mode with artificial solutions containing only clean HCl. In such conditions, only DD and MD units were in operation.

Results reproducibility was verified by performing 5 tests under the same operating conditions (WA and RA1 flowrate: 20 l h⁻¹ and 19 l h⁻¹, respectively, and WA inlet average HCl concentration: 100 g l⁻¹) for which similar concentration values of the RA1 (Std. Dev ~ 1.1 g l⁻¹) and RA2 (Std. Dev ~ 2.6 g l⁻¹) samples were obtained. Furthermore, these first tests were in line with the results carried out on a laboratory scale unit (Gueccia et al., 2020).

Two different sets of experiments were performed with HCl by changing either the waste or the recovered acid flow rate, while keeping fixed all other parameters. The initial acid concentration of 100 g l⁻¹ was kept for all the tests with hydrochloric acid.

As shown in Figure 3(a), where the WA flow rate varies from 15 to 25 l h⁻¹, an increase in the flow rate leads to an increase of the amount of acid entering the DD, therefore a higher concentration in the RA stream. As a direct consequence, the HCl concentration in the recovered acid solution exiting from MD unit (RA2) is enhanced with the WA too.

RA1 flow rate variation was also tested, by increasing the flow rate from 15 to 21 l h⁻¹. With the designed pump configuration P-RA, installed in the suction side of the DD module (see Figure 1), the designed value of 25 l h⁻¹ was not possible to be achieved due to gas suction of the pump. As shown in Figure 3(b), a RA1 flow rate increase leads to lower concentrations of acid in the RA1, and consequently in the RA2, due to a greater dilution.

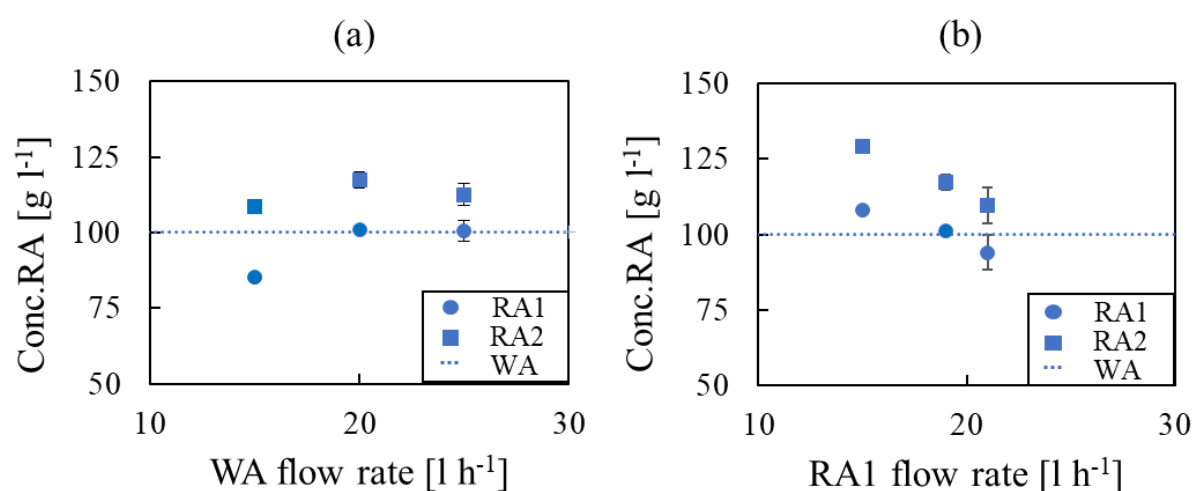


Fig. 3. HCl concentration in the recovered acid from DD (RA1, round symbols) and from the MD (RA2,

square symbols) *versus* (a) WA flow rate (RA1 flow rate = 19 l h⁻¹) and (b) RA1 flow rate (WA flow rate = 20 l h⁻¹). Dotted horizontal line: WA inlet average HCl concentration (100 g l⁻¹). Thermostatic fluid flow rate and hot / cold temperatures: 400 l h⁻¹, 60°C and 25°C. Tests with artificial HCl solutions.

Contrarily to the higher concentration values observed, the acid recovery in DD decreases from 93% to 68%, when increasing the WA flow rate, and the HCl drag over detected through the MD membrane increases from 6% to 8%, as shown in Figure 4(a), causing a deterioration in the overall performance as the WA flow rate increases.

Opposite results are obtained for the increase of the recovered acid (RA1) flowrate: an increasing trend in the RR values is observed in Figure 4(b), from 65% to 85%, with a decreasing acid drag over, from 13% to 5%.

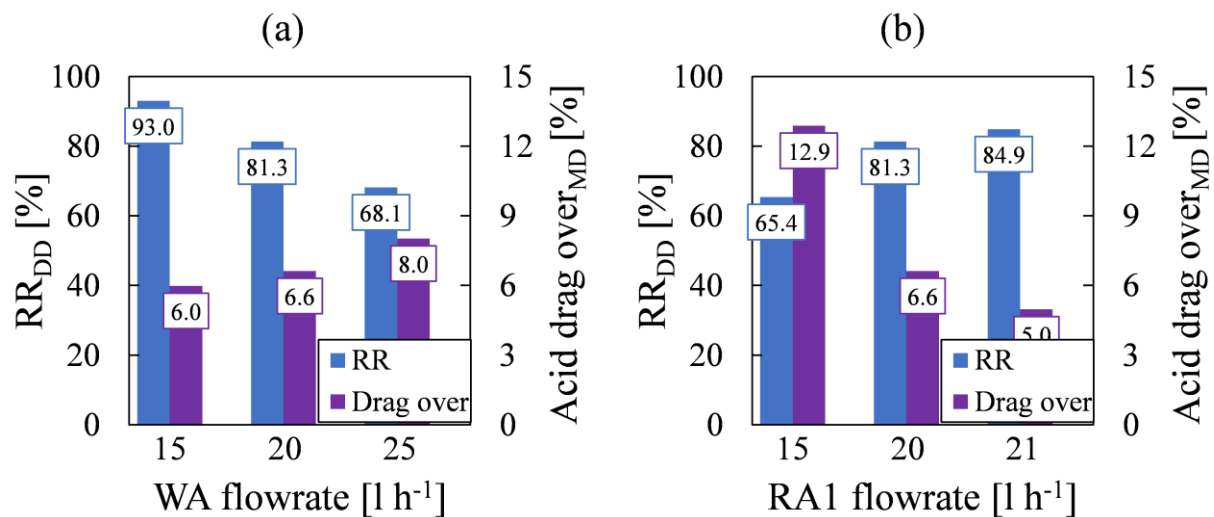


Fig. 4. DD recovery ratio and MD acid drag over *versus* (a) WA flow rate (RA1 flow rate = 19 l h⁻¹) and (b) RA1 flow rate (WA flow rate = 20 l h⁻¹). WA inlet average HCl concentration: 100 g l⁻¹. Thermostatic fluid flow rate and hot / cold temperatures: 400 l h⁻¹, 60°C and 25°C. Tests with artificial HCl solutions.

The MD performance was explored by investigating the best operating conditions for the thermostatic fluid, in terms of hot side inlet temperature and flow rate. As expected, the permeate flux (RW1 flux) increases with the increase of the thermal power, due to the increase of hot side inlet temperature and flow rate (see Figure 5(a)).

Consequently, an acid drag over through the MD membrane was observed and, as for the RW1 flux, it increases as the thermostatic flow rate increases at both the studied temperatures and

this result is more evident at the higher temperature of 70°C. In fact, as shown in Figure 5(b), drag over values up to 18% were observed at this temperature because HCl vapour pressure curve is steeper with temperature compared to water vapour pressure one.

Also the thermal performance, in terms of Gain Output Ratio (GOR), is presented for both the sets of experiments in Figure 5(c). For both temperatures the GOR, and thus the thermal efficiency of the MD unit, declines when increasing the thermostatic fluid flow rate, with a positive effect of temperature on it. In fact, values ranging from 0.29 to 0.40 and from 0.39 to 0.57 were obtained, at inlet T-fluid temperatures of 60 °C and 70 °C, respectively.

Thus, the most energy efficient conditions are at the lowest flow rate of 300 l h⁻¹ and a temperature of 70 °C.

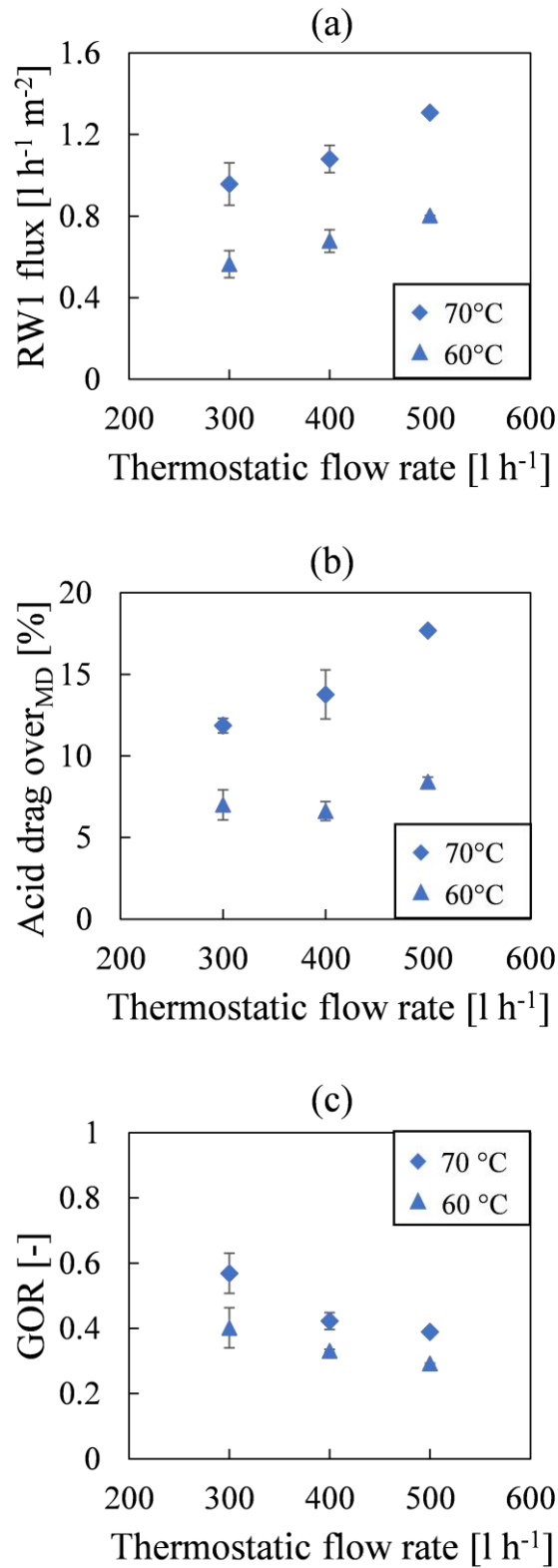


Fig. 5. (a) RW1 flux, (b) MD acid drag over and (c) GOR values *versus* thermostatic fluid flow rate at variable inlet temperature: 60 °C (triangle symbols), 70 °C (rhombic symbols). WA flow rate: 20 l h⁻¹; RA1 flowrate: 19 l h⁻¹. WA inlet average HCl concentration: 100 g l⁻¹. Thermostatic cold temperature: 25 °C. Tests with artificial HCl solutions.

Notwithstanding the thermal integration implemented inside the MD module, GOR values were all below 1 (i.e. less effective than a simple evaporation unit). This is due to MD design, oriented more to the achievement of high fluxes rather than high thermal efficiency, thanks to the fact that the thermal energy used for the MD operation is on site industrial waste heat, which is a commonly accepted approach when the thermal energy is provided by waste-heat (Christie et al., 2020).

Finally, a temperature of 60°C and a flow rate of 300 l h⁻¹ were selected as standard operating conditions in all tests performed with the real solutions, as a best tradeoff between the highest GOR and the lowest MD acid drag over.

3.2 Tests performed with HCl and FeCl₂ solutions

The first experiments with FeCl₂ and HCl solutions were performed using a purposely generated pickling solution (see Sec. 2.2), which resulted free of zinc ions. Results obtained were significantly affected by the well-known “salt effect” (Gueccia et al., 2020, 2019; Luo et al., 2013). With this respect, it is of interest noting how the HCl concentration in RA1 can even reach higher values than the WA inlet concentration (Figure 6(a)), as observed for the highest WA flow rate, and this finding can be certainly attributed to the salt effect. Similarly, higher acid recoveries than those obtained without iron salts in solution are gained due to the presence of additional chlorides, which enhances the HCl diffusion through the DD membranes. This result can be observed in Figure 6(b), where the RR for experiments performed with acid concentration of 100 g l⁻¹ and 80 g l⁻¹ of iron ions are reported as a function of WA flow rate. The highest value of RR, slightly below 90%, is observed for a WA flow rate of 20 l h⁻¹, marking an important difference with the value of 81% obtained for the sole HCl solution in the same working condition.

As regards the passage of iron through the DD membranes, an interesting result was observed when the WA flow rate is increased. In fact, despite the increase in the amount of entering iron

with the WA flow rate, a slightly lower concentration in the RA1 stream is gained (Figure 6(a)) and a significant reduction of the iron leakage through the membrane is obtained Figure 6(b)). A tradeoff between the RR and the iron leakage has to be implemented here too, thus WA and RA flow rates of 20 and 19 l h⁻¹, respectively, was adopted as standard working conditions in all subsequent tests.

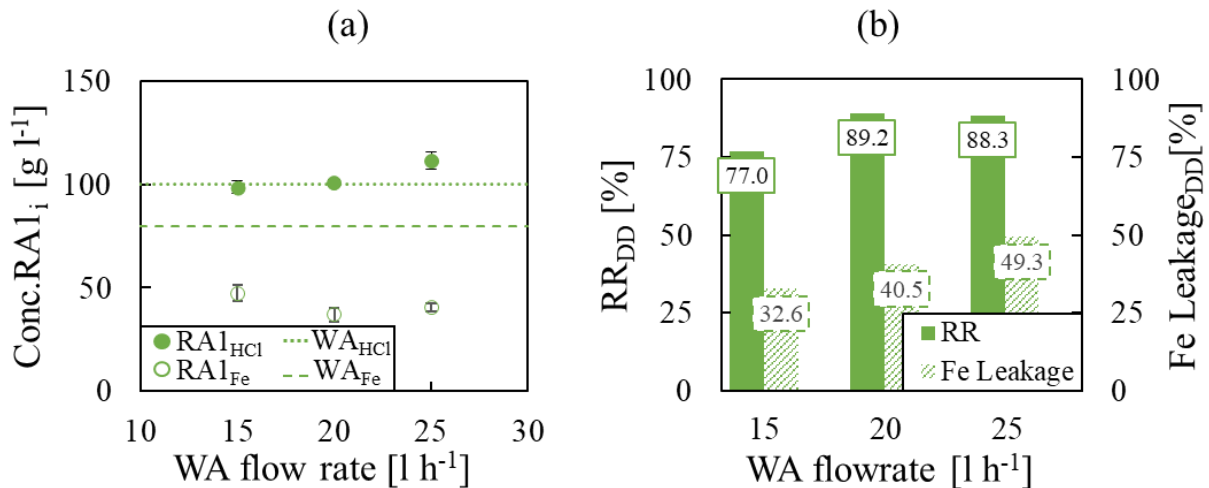


Fig. 6. (a) HCl (solid symbols) and iron (empty symbols) concentration in the recovered acid from DD and (b) DD recovery ratio (solid bar) and iron leakage (striped bar) *versus* WA flow rate (RA1 flow rate: 15, 19 and 21 l h⁻¹ corresponding to the WA flow rate of 15, 20 and 25 l h⁻¹, respectively¹). Dotted horizontal line: WA inlet average HCl concentration (100 g l⁻¹). Dashed horizontal line: WA inlet average Fe concentration (80 g l⁻¹). Tests with real solutions.

Conversely, a decline in the MD operation is observed when the iron is also present in the feed solution, as iron salts reduce the water vapor pressure and, therefore, the driving force for the passage through the membrane, leading also to a greater relative acid drag over. For the sake of brevity, quantitative results for the MD units are reported only for the final tests and presented in the following paragraph (Section 3.3 Figure 7(c)).

¹ Same flow rates for WA and RA1 were originally planned, but RA1 flow rates could not always reaches the target due to some operational limitations in the RA1 pump.

3.3 Tests performed with HCl, FeCl₂ and ZnCl₂ solutions

Finally, the presence of all the three main components of real pickling solutions was considered and two different WA cases were investigated, differing in Fe concentration, namely of 44 and 117 g l⁻¹, while keeping HCl and Zn concentration at fixed values (see Table 2).

The transport mechanism of zinc is somehow similar to the acid one as zinc forms negatively-charged chloro-complexes that can easily permeate through the DD membrane. For this reason, zinc is a “competitor” for acid permeation. As a result, the recovered acid is lower compared to what gained in the HCl+FeCl₂ tests for both cases with different iron concentrations (see Figure 7(a)). However, at the highest iron concentration (Fe concentration 117 g l⁻¹) a high acid recovery is ensured (above 82%), which is comparable with the test with HCl only, thus highlighting the importance of the salt effect in reaching high acid recovery, even in the presence of zinc.

On the other side, the iron chlorides in solution also result in a higher zinc leakage as their concentration increases (Figure 7(b)). However, the low concentration of zinc in solution allows to manage the closed-loop operation of the whole system, keeping the required small concentration of zinc in the RA2 in order to avoid the accumulation of this component in the pickling tank (Culcasi et al., 2019).

Iron leakage is significantly higher than expected. In fact, results previously obtained in a laboratory dialyzer, with same configuration and operating conditions indicated an iron leakage of about 30% and a leakage of 60% for zinc (Gueccia et al., 2020), while values up to 40% and 65%, respectively, are observed here. This could be attributed to the position of the P-RA pump at the suction side of the DD, which resulted in a higher differential pressure along the two sides of the DD unit and, therefore, in a hydraulic leakage from the feed to the draw channels. Moreover, the residence time in the pilot configuration is higher (laboratory dialyzer residence time is around 4 min compared to the 7 minutes of the pilot) thus providing additional time for

the metals to diffuse from the concentrate to the dilute side, while marginal benefits are provided to the acid recovery, given the already high values achieved, which can hardly be increased by a longer residence time. Thus an optimized geometry would require a significantly lower membrane area, which could reduce the metals leakage without affecting the recovery of acid.

The MD performances suffer significantly as the salts concentration increases in the RA1 solution, likely due two main facts: increase of the molar HCl flux through the MD membranes, on one side, and reduction of the water vapor permeation, on the other. In fact, contrarily to the ideal Raoult's law, which would predict a vapor pressure reduction for both volatile components, it is observed that when a salt is dissolved in a mixture of water and acid, the presence of salt enhances the acid vapour pressure, while it reduces water one (Johnson and Furter, 1960; Tomaszewska et al., 1998). This is known as "salting out" effect, which typically results in a higher acid drag over through the microporous MD membranes as showed in Figure 7(c).

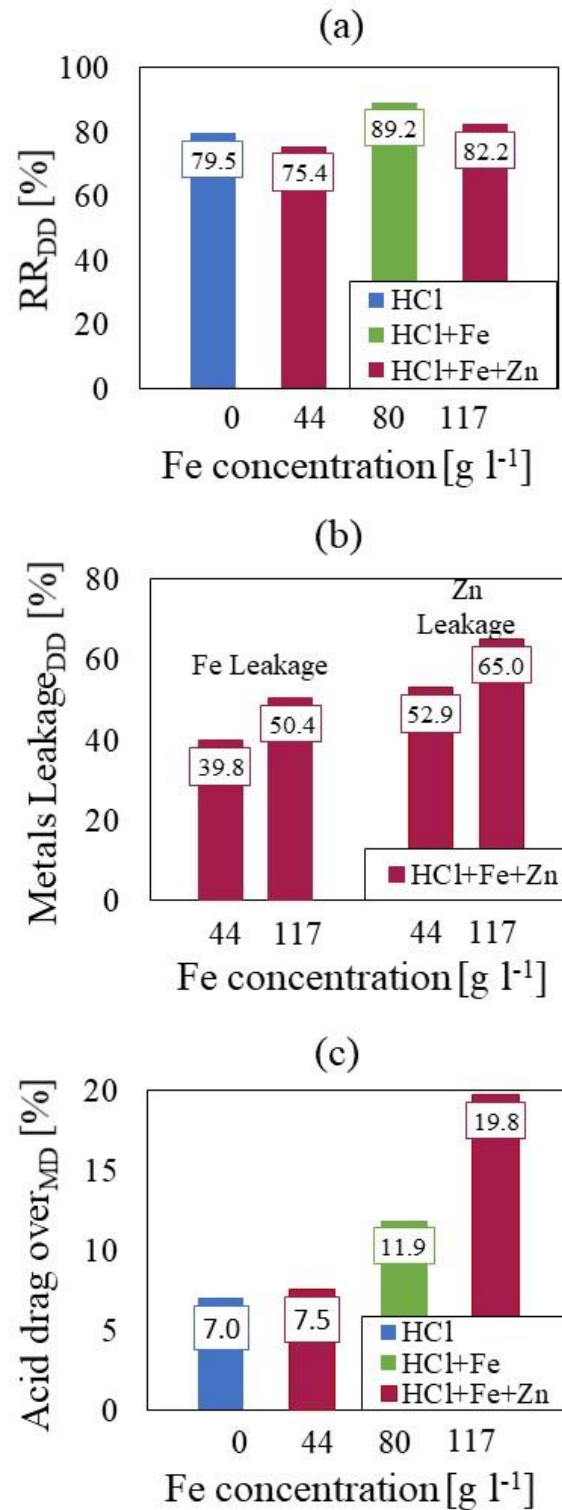


Fig. 7. (a) DD recovery ratio, (b) DD metals leakage and (c) MD acid drag over *versus* iron concentration. WA inlet average HCl concentration: 100 g l⁻¹. WA inlet average Zn concentration (for the two tests with HCl+Fe+Zn): 8 g l⁻¹. WA flow rate: 20 l h⁻¹; RA1 flowrate: 19 l h⁻¹. Thermostatic fluid flow rate and hot / cold temperatures: 300 l h⁻¹, 60°C and 28°C. Tests with real solutions.

A polypropylene cooled CSTR unit is used for these latter tests to separate and selectively recover the two metal components. Previous laboratory tests had shown that a selective

precipitation is possible by controlling the solution pH, since Fe (III) hydroxide precipitation pH is in the range of 2-3, while zinc insoluble salts (e.g. $Zn(OH)_2$) precipitate above the range 6-7. Therefore, to accomplish the iron separation in the CSTR section, hydrogen peroxide and ammonia hydroxide are fed in order to oxidize Fe (II) to Fe (III) and to precipitate iron hydroxide, respectively. All the tests were performed by keeping a constant pH=4 in the CSTR and a redox potential set-point at 300mV (in practice, ranging from 250 to 400 mV), which ensures a complete iron oxidation. Interestingly, a purity of 99% was obtained for the iron hydroxide solid separated after filtration. The choice of using ammonia hydroxide as alkaline reactant, though not being most cost-effective and environmental advantageous option, allows to create a by-product stream consisting in a zinc/ammonium chloride solution, which can be used in the fluxing step of the hot-dip galvanizing chain. Thus, the new recycling process here proposed does not create any waste stream to be disposed nor requires extra quantity of chemicals compared to the state-of-the-art processes.

3.4 Long time pilot system performance

For the implementation of the central process control system, an industrial-type PLC was chosen in order to achieve the maximum level of process reliability and robustness.

Results of the long-time automatic mode operations for the three different main sections are reported in following graphs to prove the continuous operations and performance of the demonstrator.

In Figure 8, double plots are shown to visualize the conductivities and flow rates in the DD unit for a whole day of operation (7 hours). Typical conductivity profiles during DD backflush operation are detectable. DD backflush cycle typically lasts 2 minutes with a 2-hours frequency. The system has the ability to respond quickly to variations as can be seen after every backflush and for flow rate variations (e.g. after 4.3 hours, the waste acid flowrate increases from 20 to 25 l h⁻¹).

The sub-atmospheric pressure in the DD diffusate channel leads to the formation of gas bubbles exiting with the diffusate of the DD module, entering the pump and MD module, respectively. Consequently, flow sensors, which are very sensitive to gas bubbles, gave values with strong fluctuations.

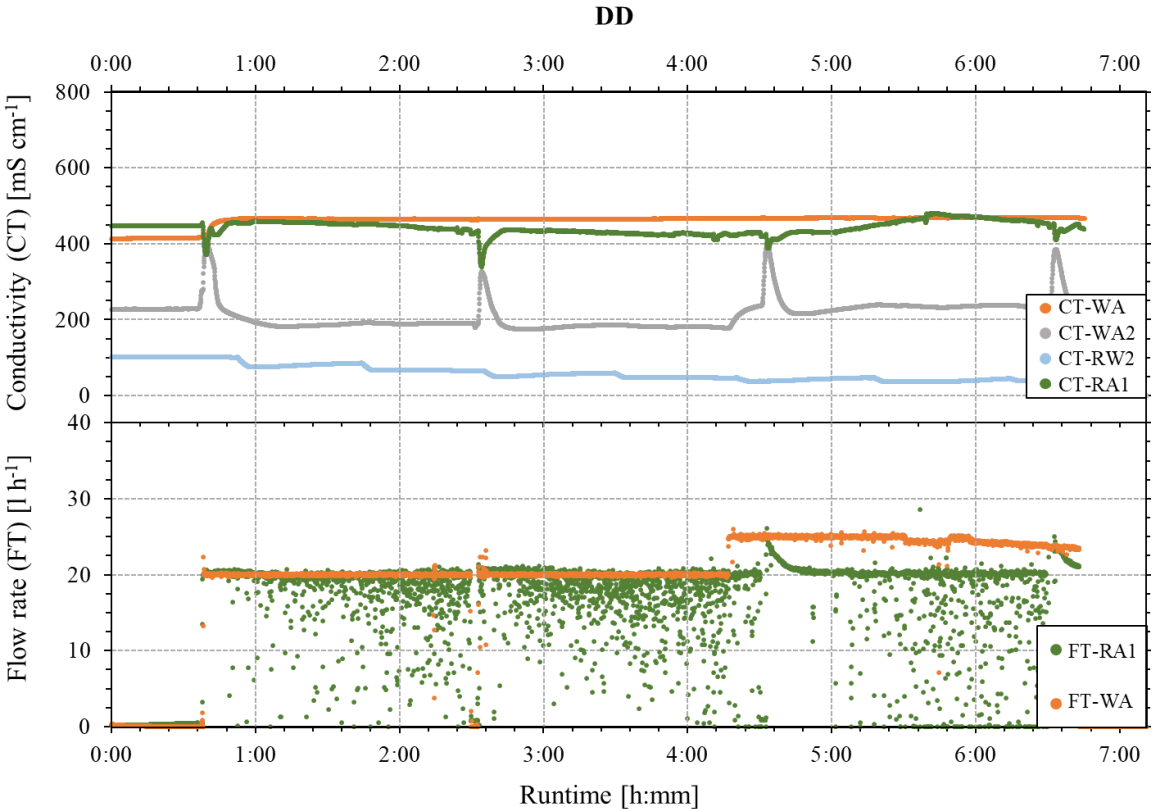


Fig. 8. Long-run DD operation. Conductivities values (top) and flow rates (bottom) *versus* operation time. Tests with real HCl solution. WA inlet HCl, Fe and Zn concentration: 100, 44, 8 g l⁻¹, respectively.

A further demonstration of the system stability is shown in Figure 9, where variations of flow rate and temperatures in the MD thermostatic line are reported.

An emergency shut-down is also noticeable in Figure 9 (after 4 hours of operation, which is restored at around 5 hours), with streams flow rate suddenly going to zero and a slight ramp down in the temperature profiles.

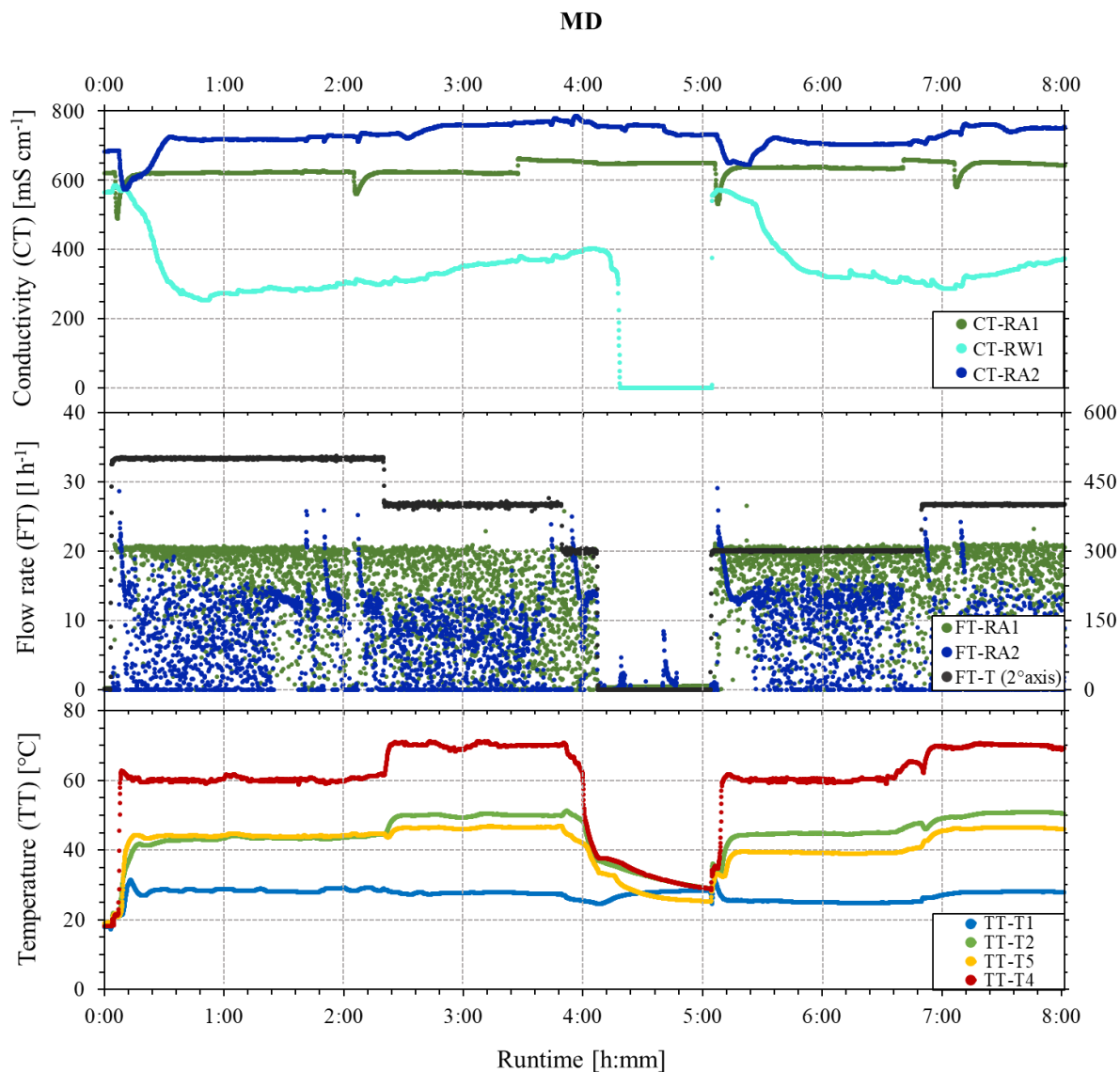


Fig. 9. Long-run MD operation. Conductivities values (top), flow rates (middle) and temperatures (bottom) *versus* operation time. Tests with artificial HCl solution. WA inlet HCl concentration: 100 g l⁻¹.

Finally, an example of control system action in the CSTR is reported in Figure 10. The set points of pH and redox potential are of 4 and 300 mV, respectively. The oxidant and reactants flow rates are automatically adjusted in order to control the set points values. In addition, the slurry temperature in the precipitation unit is controlled by adjusting the cooling water flow rate in the heat exchanger (temperature does not exceed the maximum set value of 35°C).

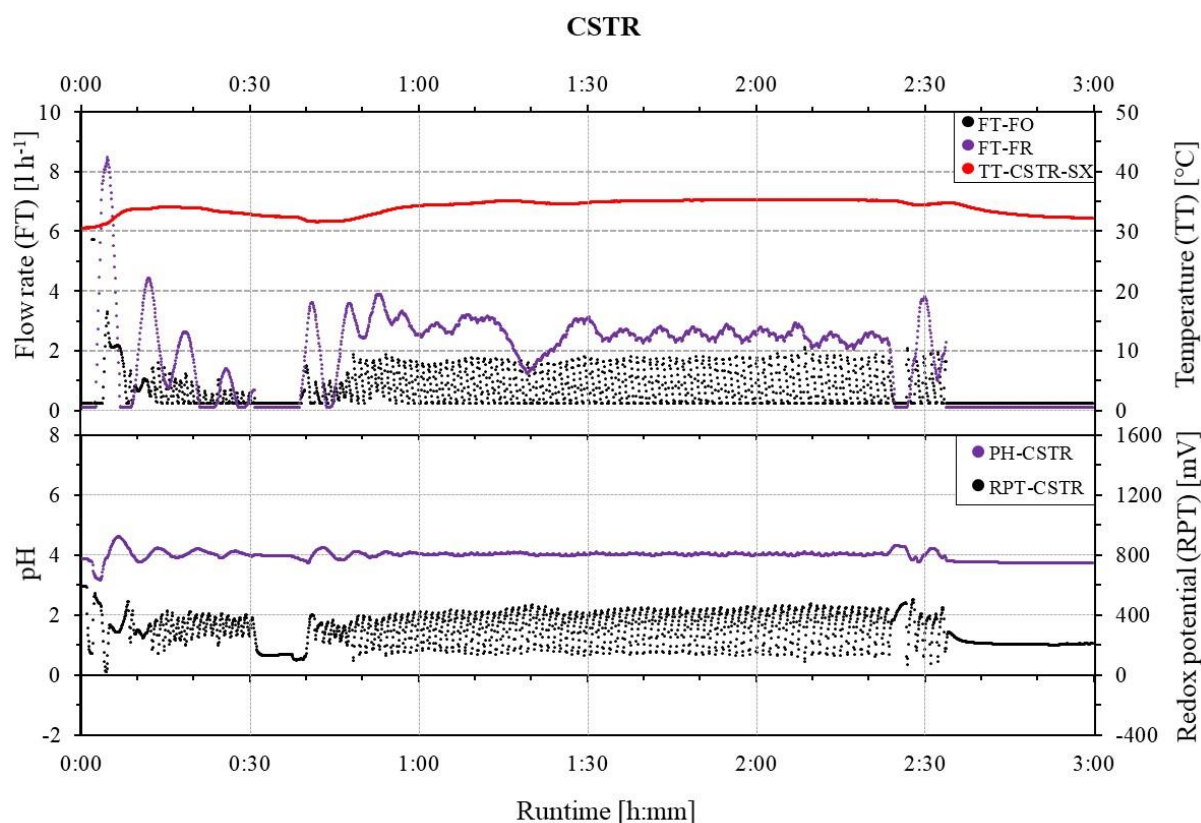


Fig. 10. Long-run CSTR operation. Flow rates (top) and pH and redox potential values (bottom) *versus* operation time. Tests with real HCl solutions. WA inlet HCl, Fe and Zn concentration: 100, 117, 8 g l⁻¹, respectively.

4 CONCLUSIONS

Operational results of a pilot plant for the treatment and valorisation of pickling solution are presented. Membrane separation processes (DD and MD) and reactive precipitation have been integrated in order to accomplish a continuous acid regeneration and iron / zinc separation, thus allowing to keep the pickling bath at a higher performance level, recover valuable solid by-products, avoid any waste stream to be disposed and implementing a fully circular reuse of the process streams.

The pilot plant was commissioned and operated in a real industrial environment using first artificial HCl solutions and then real pickling liquors.

The highest acid recovery, nearly 90%, was observed for the HCl+ FeCl₂ thanks to the “iron salt effect”, which enhances Cl⁻ permeation. Conversely, lower acid recoveries (~80%) were

observed when also zinc is present in solution, as it acts as competitor for the acid permeation due to the negatively-charged zinc chloro-complexes. High values of iron leakage through the DD unit were observed (over 50%), especially if compared to literature findings, indicating values below 30%. The high Fe passage here is a consequence of long residence times in the DD module and hydraulic leakage caused by the suction position of the P-RA pump. Quantitative separation of iron and zinc has been demonstrated in the CSTR unit, with a solid iron hydroxide of 99% purity and a zinc / ammonium chloride solution obtained as fluxing bath for the hot-dip galvanizing process.

Finally, notwithstanding the importance of using waste-heat driven MD for the overall process energy sustainability, an important drop in MD performance is observed due to high volatility of HCl and detrimental “salting out” effect due to the presence of salts depressing water vapour pressure.

Overall operational results have shown that acid can be successfully recovered and re-concentrated, iron salt recovered in the form of marketable hydroxides and fluxing solution eventually obtained from the outlet of the iron crystalliser. Both acid and fluxing solution can be recirculated into the plant.

High level of system reliability and robustness has been achieved by the implementation of an industrial-type central process control system.

Results of the long-time automatic mode operations have proven the continuous operations and performance of the demonstrator.

Further developments and investigations are suggested to improve DD membrane selectivity against Fe and Zn and module integrity, which have caused part of the stated leakage. Moreover, an optimized configuration should aim at reduced residence time in the DD unit and a relocation of the P-RA pump to minimize hydraulic leakage. This could reduce the metals leakage in the DD diffusate, consequently improving the MD operation as well.

A further optimization step on the process set-up and operating conditions will allow the technology to reach a competitiveness level enabling it to enter into the metal processing market for a further step towards sustainability.

ACKNOWLEDGMENTS

This work was supported by the EU within ReWaCEM project (Resource recovery from industrial Wastewater by Cutting Edge Membrane technologies, Horizon 2020 program [grant number. 723729]).

The authors are grateful to DEUKUM GmbH and Solar Spring, for proving and supporting the pilot construction, assembly and operation, and to Tecnozinco SrL, for hosting the pilot and supporting installation and operation activities.

Nomenclature, acronyms and units

AEM	Anion Exchange Membrane
BAT	Best Available Technologies
CSTR	Continuous Stirred Tank Reactor
CT	Conductivity Transmitter
CW	Cooling Water
DD	Diffusion Dialysis
EU	European Union
FGAGMD	Feed Gap Air Gap Membrane Distillation
FO	Fresh Oxidant
FR	Fresh Reactant
FT	Flow Transmitter
FW	Fresh Water
GOR	Gain Output Ratio

H		Electric Heater
HMI		Human Machine Interface
HW		Heating Water
HX		Heat Exchanger
MD		Membrane Distillation
P		Pump
PFD		Process Flow Diagram
PLC		Programmable Logic Controller
PT		Pressure Transmitter
RA		Recovered Acid
RW		Recovered Water
S		Slurry
SPS		Spent Pickling Solution
T		Thermostatic
theor		theoretical
TT		Temperature Transmitter
WA		Waste Acid
A	[m ²]	area
c	[g l ⁻¹]	mass concentration
cp	[kJ kg ⁻¹ K ⁻¹]	specific heat
conductivity	[mS cm ⁻¹]	conductivity
F	[l h ⁻¹]	volumetric flow rate
flux	[l h ⁻¹ m ⁻²]	flux
h_v	[kJ kg ⁻¹]	enthalpy of evaporation
m	[g]	mass

\dot{Q}	[kJ]	heating power
RPT	[mV]	redox potential
RR	[%]	recovery ratio
T	[°C]	temperature
ρ	[g l ⁻¹]	density

REFERENCES

- Agrawal, A., Sahu, K.K., 2009. An overview of the recovery of acid from spent acidic solutions from steel and electroplating industries. *J. Hazard. Mater.* 171, 61–75. <https://doi.org/10.1016/j.jhazmat.2009.06.099>
- Andritz Metals, n.d. Regeneration systems for hydrochloric waste pickling solutions [WWW Document]. URL <https://www.andritz.com/products-en/group/metals/carbon-steel-regeneration/hydrochloric-plant>
- Balakrishnan, M., Batra, R., Batra, V.S., Chandramouli, G., Choudhury, D., Hälbig, T., Ivashechkin, P., Jain, J., Mandava, K., Mense, N., Nehra, V., Rögener, F., Sartor, M., Singh, V., Srinivasan, M.R., Tewari, P.K., 2018. Demonstration of acid and water recovery systems: Applicability and operational challenges in Indian metal finishing SMEs. *J. Environ. Manage.* 217, 207–213. <https://doi.org/10.1016/j.jenvman.2018.03.092>
- Bascone, D., Cipollina, A., Morreale, M., Randazzo, S., Santoro, F., Micale, G., 2016. Simulation of a regeneration plant for spent pickling solutions via spray roasting. *Desalin. Water Treat.* 57, 23405–23419. <https://doi.org/10.1080/19443994.2015.1137146>
- Campano, B.R., 2012. The Kleingarn Regenerated Spent Acid at Increasing Ferrous (Fe⁺²) and Ferric (Fe⁺³) Chloride Content.
- Christie, K.S.S., Horseman, T., Lin, S., 2020. Energy efficiency of membrane distillation: Simplified analysis, heat recovery, and the use of waste-heat. *Environ. Int.* 138, 105588. <https://doi.org/10.1016/j.envint.2020.105588>
- Culcasi, A., Gueccia, R., Randazzo, S., Cipollina, A., Micale, G., 2019. Design of a novel membrane-integrated waste acid recovery process from pickling solution. *J. Clean. Prod.* 236, 117623. <https://doi.org/10.1016/j.jclepro.2019.117623>
- Devi, A., Singhal, A., Gupta, R., Panzade, P., 2014. A study on treatment methods of spent pickling liquor generated by pickling process of steel. *Clean Technol. Environ. Policy* 16, 1515–1527. <https://doi.org/10.1007/s10098-014-0726-7>
- Drioli, E., Wu, Y., Calabro, V., 1987. Membrane distillation in the treatment of aqueous solutions. *J. Memb. Sci.* 33, 277–284. [https://doi.org/10.1016/S0376-7388\(00\)80285-9](https://doi.org/10.1016/S0376-7388(00)80285-9)
- European Commission, 2006. Control Reference Document on Best Available Techniques for the Surface Treatment of Metals and Plastics.
- Frias et al., 1997. Novel process to recover by-products from the pickling baths of stainless steel. Proj. Funded by Eur. Community under Ind. Mater. Technol. Program. (Brite-Euram III), Proj. BE-3501, Contract BRPR-CT 97-0407. https://doi.org/https://cordis.europa.eu/project/rcn/37577_en.xml
- Gueccia, R., Aguirre, A.R., Randazzo, S., Cipollina, A., 2020. Diffusion Dialysis for

- Separation of Hydrochloric Acid , Iron and Zinc Ions from Highly Concentrated Pickling Solutions. *Membranes (Basel)*. 10, 1–17.
<https://doi.org/https://doi.org/10.3390/membranes10060129>
- Gueccia, R., Randazzo, S., Chillura Martino, D., Cipollina, A., Micale, G., 2019. Experimental investigation and modeling of diffusion dialysis for HCl recovery from waste pickling solution. *J. Environ. Manage.* 235, 202–212.
<https://doi.org/10.1016/j.jenvman.2019.01.028>
- Harris, L.J.F., 1994. Introduction to spray roasting process for hydrochloric acid regeneration and its application to mineral processing. *Hydrometall.* '94 923–937.
https://doi.org/10.1007/978-94-011-1214-7_62
- Jatuphaksamphan, Y., Phinichka, N., Prapakorn, K., Supradist, M., 2010. Pickling Kinetics of Tertiary Oxide Scale Formed on Hot-Rolled Steel Strip. *J. Met. Mater. Miner.* 20, 33–39.
- Johnson, A.I., Furter, W.F., 1960. Salt effect in vapor-liquid equilibrium, part II. *Can. J. Chem. Eng.* 38, 78–87. <https://doi.org/10.1002/cjce.5450380304>
- Jung Oh, S., Moon, S.H., Davis, T., 2000. Effects of metal ions on diffusion dialysis of inorganic acids. *J. Memb. Sci.* 169, 95–105. [https://doi.org/10.1016/S0376-7388\(99\)00333-6](https://doi.org/10.1016/S0376-7388(99)00333-6)
- Kerney, U., 1994. Treatment of spent pickling acids from hot dip galvanizing. *Resour. Conserv. Recycl.* 10, 145–151. [https://doi.org/10.1016/0921-3449\(94\)90047-7](https://doi.org/10.1016/0921-3449(94)90047-7)
- Kleingarn, J.P., 1988. Pickling in hydrochloric acid, in: *Intergalva, EGGA European General Galvanizers Association*. p. GF2/1-13.
- Kobuchi, Y., Motomura, H., Noma, Y., Hanada, F., 1986. Application of ion exchange membranes to the recovery of acids by diffusion dialysis. *J. Memb. Sci.* 27, 173–179.
[https://doi.org/10.1016/S0376-7388\(00\)82054-2](https://doi.org/10.1016/S0376-7388(00)82054-2)
- Kong, G., White, R., 2010. Toward cleaner production of hot dip galvanizing industry in China. *J. Clean. Prod.* 18, 1092–1099. <https://doi.org/10.1016/j.jclepro.2010.03.006>
- Luo, J., Wu, C., Wu, Y., Xu, T., 2013. Diffusion dialysis of hydrochloric acid with their salts: Effect of co-existence metal ions. *Sep. Purif. Technol.* 118, 716–722.
<https://doi.org/10.1016/j.seppur.2013.08.014>
- Luo, J., Wu, C., Wu, Y., Xu, T., 2011. Diffusion dialysis processes of inorganic acids and their salts: The permeability of different acidic anions. *Sep. Purif. Technol.* 78, 97–102.
<https://doi.org/10.1016/j.seppur.2011.01.028>
- Marañón, E., Fernández, Y., Suárez, F.J., Alonso, F.J., Sastre, H., 2000. Treatment of acid pickling baths by means of anionic resins. *Ind. Eng. Chem. Res.* 39, 3370–3376.
<https://doi.org/10.1021/ie0000414>
- Palatý, Z., Žáková, A., 2006. Competitive transport of hydrochloric acid and zinc chloride through polymeric anion-exchange membrane. *J. Appl. Polym. Sci.* 101, 1391–1397.
<https://doi.org/10.1002/app.22748>
- Regel, M., Sastre, A.M., Szymanowski, J., 2001. Recovery of zinc(II) from HCL spent pickling solutions by solvent extraction. *Environ. Sci. Technol.* 35, 630–635.
<https://doi.org/10.1021/es001470w>
- Schwantes, R., Seger, J., Bauer, L., Winter, D., Hogen, T., Koschikowski, J., Geißen, S.U., 2019. Characterization and assessment of a novel plate and frame md module for single pass wastewater concentration–feed gap air gap membrane distillation. *Membranes (Basel)*. 9. <https://doi.org/10.3390/membranes9090118>
- Stocks, C., Wood, J., Guy, S., 2005. Minimisation and recycling of spent acid wastes from galvanizing plants. *Resour. Conserv. Recycl.* 44, 153–166.
<https://doi.org/10.1016/j.resconrec.2004.11.005>
- Strathmann, H., 2004. Ion Exchange Membrane Separation Processes, in: *Membrane Science and Technology Series*. Elsevier B.V., Amsterdam, The Netherlands, pp. 205–212.

- Tomaszewska, M., Gryta, M., Morawski, A.W., 2001. Recovery of hydrochloric acid from metal pickling solutions by membrane distillation. *Sep. Purif. Technol.* 22–23, 591–600. [https://doi.org/10.1016/S1383-5866\(00\)00164-7](https://doi.org/10.1016/S1383-5866(00)00164-7)
- Tomaszewska, M., Gryta, M., Morawski, A.W., 1998. The influence of salt in solutions on hydrochloric acid recovery by membrane distillation. *Sep. Purif. Technol.* [https://doi.org/10.1016/S1383-5866\(98\)00073-2](https://doi.org/10.1016/S1383-5866(98)00073-2)
- Tongwen, X., Weihua, Y., 2003. Industrial recovery of mixed acid (HF + HNO₃) from the titanium spent leaching solutions by diffusion dialysis with a new series of anion exchange membranes. *J. Memb. Sci.* 220, 89–95. [https://doi.org/10.1016/S0376-7388\(03\)00218-7](https://doi.org/10.1016/S0376-7388(03)00218-7)
- Xu, J., Lu, S., Fu, D., 2009. Recovery of hydrochloric acid from the waste acid solution by diffusion dialysis. *J. Hazard. Mater.* 165, 832–837. <https://doi.org/10.1016/j.jhazmat.2008.10.064>
- Zhao, B., Zhang, Y., Dou, X., Yuan, H., Yang, M., 2015. Granular ferric hydroxide adsorbent for phosphate removal: Demonstration preparation and field study. *Water Sci. Technol.* 72, 2179–2186. <https://doi.org/10.2166/wst.2015.438>